Spectroscopy of the cation distribution in the schorlomite species of garnet

Andrew Locock, Robert W. Luth

Department of Geology, University of Alberta, Edmonton, Alberta T6G 2E3, Canada

Ronald G. Cavell

Department of Chemistry, University of Alberta, Edmonton, Alberta T6G 2E1, Canada

Dorian G. W. Smith

Department of Geology, University of Alberta, Edmonton, Alberta T6G 2E3, Canada

M. John M. Duke

SLOWPOKE Reactor Facility, University of Alberta, Edmonton, Alberta T6G 2E1, Canada

Abstract

A homogeneous megacryst of schorlomite was investigated to determine the valence states of Fe and Ti and the crystallographic sites occupied by these elements. The chemical composition of the specimen was analyzed by electron microprobe, wet-chemical analysis, FTIR, and INAA. The results from X-ray absorption near-edge structure spectroscopy (XANES) are consistent with exclusively Ti^{4+} occupying the octahedral site only. The tetrahedral site is deficient in Si and the results of low-temperature ^{57}Fe Mössbauer spectroscopy indicate that the remainder of the site is occupied by Fe^{3+} and substantial Fe^{2+}. A spin-allowed intensified crystal-field transition of $^{[4]}Fe^{2+}$ is present in the near-infrared spectrum. The optical absorption spectrum is dominated by an intense band centered at 500 nm with a full width of 8000 cm^{-1} at half maximum peak height; this band is assigned to an Fe^{2+}-Ti^{4+} intervalence charge transfer transition between $^{[4]}Fe^{2+}$ and $^{[6]}Ti$. The cation site occupancies in this specimen of schorlomite can be expressed by the following formula: $\{Ca_{2.866}Mg_{0.080}Na_{0.038}Mn_{0.019}\}_{\Sigma 3.003}[Ti^{4+}_{1.058}Fe^{3+}_{0.631}Al_{0.137}Fe^{2+}_{0.057}Mg_{0.055}Zr_{0.039}V^{3+}_{0.014}Mn_{0.013}]_{\Sigma 2.004}$-$(Si_{2.348}Fe^{3+}_{0.339}Fe^{2+}_{0.311}[4H]_{0.005})_{\Sigma 3.003}O_{12}$.

Introduction

The general formula of silicate garnets may be written $\{X\}_3[Y]_2(Si)_3O_{12}$ where { } represents triangular dodecahedral coordination, [ ] indicates octahedral coordination, and ( ) denotes tetrahedral coordination (Hawthorne, 1981; Leigh, 1990). The garnet structure usually crystallizes in the cubic space group $Ia3d$.

Schorlomite is a species of silicate garnet containing more than one atom of Ti per formula unit. Melanite is the complementary varietal name for titanian andradite that has <1 Ti atom per formula unit (Deer et al., 1982). Unlike most other natural silicate garnets the tetrahedral site in schorlomite is not fully occupied by Si. This deficiency, together with the large concentrations of Ti and both Fe^{3+} and Fe^{2+} in the mineral, has given rise to contention about the cation distribution among the crystallographic sites in schorlomite. Numerous studies have investigated the crystal chemistry of schorlomite and titanian andradite in attempts to resolve the roles of Ti and Fe. The results of chemical studies have shown an inverse correlation between Si and Ti and have been used as evidence that Ti^{4+} replaces Si^{4+} in the tetrahedral site, with any excess Ti allocated to the octahedral site (often as Ti^{3+}) (Koenig, 1886; Hoffmann, 1902; Howie and

Woolley, 1968; Basso et al., 1981; Onuki et al., 1981; Dingwell and Brearley, 1985; Sawaki, 1988; Lueck and Russell, 1994). Optical and near-infrared spectroscopic studies have produced several interpretations of the crystal chemistry of schorlomite including $^{[6]}Ti^{3+}$ (Manning and Harris, 1970; Moore and White, 1971), $^{[4]}Fe^{2+}$ (Manning and Harris, 1970; Dowty, 1971; Huggins et al., 1977b; Smith, 1978), and various charge-transfer mechanisms (Dowty, 1971; Moore and White, 1971; Huggins et al., 1977b). From the numerous ^{57}Fe Mössbauer studies of schorlomite no consensus has been reached about the distribution of Fe (and indirectly Ti). Interpretations have included $^{[4]}Ti^{4+}$ in slight amounts (Huggins et al., 1977b; Koritnig et al., 1978; Kühberger et al., 1989), slight quantities of $^{[6]}Ti^{3+}$ (Huggins et al., 1977b; Schwartz et al., 1980; Onuki et al., 1982; Wu and Mu, 1986; Kühberger et al., 1989), exclusive $^{[6]}Ti^{4+}$ (Dowty, 1971; Amthauer et al., 1977), significant $^{[4]}Fe^{2+}$ (Dowty, 1971; Huggins et al., 1977b; Amthauer et al., 1977; Koritnig et al., 1978; Kühberger et al., 1989) and various charge-transfer or electron-delocalization mechanisms (Huggins et al., 1977b; Schwartz et al., 1980; Yupu and Ruiying, 1985; Wu and Mu, 1986).

Most of the above studies indirectly constrained the

valence states and site distribution of Ti by using general crystal-chemical guidelines and by determining the site occupancies and oxidation states of the other constituent cations (usually Fe). Stoichiometric constraints were then used to fix the distribution of Ti and its valence states. This approach, which assumes perfect stoichiometry, propagates all the analytical uncertainties into the calculation of the Ti distribution.

Studies using X-ray absorption near-edge structure spectroscopy (XANES) that investigated directly the coordination and valence state of Ti in schorlomite concluded that Ti was exclusively tetravalent and octahedrally coordinated within experimental error (Waychunas, 1987; de Groot et al., 1992).

There are several analytical difficulties involved in investigating schorlomite or titanian andradite. Customary wet-chemical determination of the Fe^{2+} content is hampered by the relative insolubility of garnet and gives misleading results in the presence of other reduced cations such as V^{3+} and Ti^{3+} (Groves, 1937). Optical and near-infrared spectral assignments may be equivocal because of the presence of several different transition metals. The results of ^{57}Fe Mössbauer spectroscopy may be difficult to evaluate because of the possibility of differing recoil-free fractions between the disparate crystallographic sites, as well as the variation of the hyperfine parameters with temperature and composition. Perhaps the most serious analytical challenge is the compositional zoning found in many garnet specimens; if present, this zoning precludes rational characterization of a sample by analytical methods requiring bulk portions.

This study used several analytical techniques to investigate aliquots of a single homogeneous megacryst of schorlomite. Methods included optical microscopy, powder X-ray diffractometry (XRD), electron microprobe analysis, instrumental neutron activation analysis (INAA), synchrotron-based X-ray absorption near-edge structure spectroscopy (XANES), volumetric Fe^{2+} determination, Fourier transform infrared spectroscopy (FTIR), ^{57}Fe Mössbauer spectroscopy (at 295 and 80 K), and optical absorption spectroscopy. These techniques are more fully described below. A multi-analytical approach provides mutually supporting evidence, thereby increasing the confidence of the interpretations. The valence states and site occupancies of Ti and Fe in schorlomite are the major concerns addressed by this study.

MATERIAL AND METHODS

An anhedral schorlomite megacryst was collected from the melteigite unit of the Ice River alkaline complex, Yoho National Park, British Columbia, Canada. The specimen is opaque and pitch black at thicknesses >20 μm, and it has an adamantine luster. A strong red-brown color is evinced by sections thinner than 20 μm. No zoning was observed by transmitted or reflected light microscopy. Density measurements were determined using a VDF torsion balance and toluene as an immersion liquid. The index of refraction of the sample was measured using fresh Cargille Laboratories immersion liquids and standard immersion techniques.

To prepare a purified mineral separate, schorlomite fragments were ground in a tungsten carbide swing mill with carbon dioxide pellets (to prevent oxidation). The resulting material was dry-sieved, and the size fraction collected between 120 and 170 mesh (U.S.) and washed with acetone. Impurities (apatite, biotite, calcite, diopside, nepheline, and pyrite) were removed from this size fraction by settling in diiodomethane followed by magnetic separation. The purity of the mineral separate was estimated to be >99.9%.

To estimate the end-member of schorlomite containing Fe^{3+} only, a doubly polished wafer and an aliquot of the sample powder were placed into individual alumina crucibles and heated in air for 594 h at 1050 °C. The resulting samples were investigated using Mössbauer, optical, and infrared spectroscopic methods and X-ray powder diffraction techniques.

X-ray powder diffraction

An aliquot of the purified unheated separate was prepared for X-ray diffraction by grinding it in an alumina ball mill with carbon dioxide pellets. An X-ray powder diffraction pattern from 2 to 90° 2θ was recorded on a Rigaku Geigerflex automated powder diffractometer using Co radiation, a graphite monochromator, and a scan speed of 0.6° 2θ/min. With these data the unit-cell dimension was calculated using the least-squares program of Appleman and Evans (1973), as revised for the microcomputer by Benoit (1987). The uncertainty in the X-ray peak positions is estimated to be 0.003° 2θ, on the basis of repeated scans of a quartz standard.

Microprobe analyses

Analyses were performed using an ARL SEMQ microprobe with a Tracor Northern 5600 automation package. Following preliminary examination by energy-dispersive analysis, elemental analyses were performed using the wavelength-dispersive mode, with an excitation voltage of 15 kV, a probe current of 12 nA, and beam diameter of 1 μm rastered over a 100-μm^2 area. Peak and background counting times were 20 and 10 s, respectively. Standards used included kaersutite (Na), pyrope (Mg, Al, Si), grossular (Ca), rutile (Ti), willemite (Mn), chromite (Fe), and zircon (Zr). V was the only other element observed in the energy-dispersive spectrum and was quantified with reference to a V metal standard. These microprobe results for V were subsequently shown to be consistently higher by ~50% than those from duplicate ICP and INAA analyses (on separate aliquots from the same megacryst) and are therefore not presented. Reduction of data was carried out with the use of Phi-Rho-Z program included with the Tracor Northern software. Total Fe was calculated as Fe^{3+}. Thirty-three quantitative analyses were acquired at 250-μm intervals along a traverse.

Instrumental neutron activation analysis (INAA)

Selected minor and trace elements were determined by instrumental neutron activation analysis of two aliquots of the purified schorlomite separate. Short-lived radionuclides were determined by irradiating a 30-mg aliquot for 5 min at a nominal thermal neutron flux of 1×10^{11} n/(cm²s) in an inner site of the SLOWPOKE II nuclear reactor at the University of Alberta. The irradiated sample was counted for 5 min of live time at a sample to detector distance of 6 cm after a 20-min decay period. For the determination of the long-lived radionuclides, a 500-mg aliquot was irradiated for 2 h at 10^{12} n/(cm²s). This aliquot was counted twice: initially for 50 min at a sample to detector distance of 3 cm following a decay of 6 d, and a second time for 6.94 h at a geometry of 1 cm after a total decay of 21 d. All measurements were performed in a Pb cave 10 cm thick with a graded shield of Cu and Perspex.

The γ-ray spectroscopy system included a hyperpure Ge detector with 20% efficiency [that has a full width at half maximum peak height (FWHM) of 1.9 keV for the 1332.5-keV photopeak of ^{60}Co] coupled to a microcomputer-based multichannel analyzer. Elemental concentrations were determined by the semiabsolute method of NAA (Bergerioux et al., 1979). Comparative reference materials included USGS BCR-1 (basalt), USGS W-1 (diabase), USGS RGM-1 (rhyolite), NIST NBS 1633a (fly ash), and GIT-IWG AC-E (microgranite).

X-ray absorption near-edge structure spectroscopy

Table 1 lists the minerals used as model compounds in this study. The samples were ground finely, and those for transmission studies were intimately mixed with boron nitride and mounted with Mylar tape onto sample holders. The sample for fluorescence study was mounted directly onto Mylar. Absorption spectra of the TiK and VK edges were acquired at room temperature using the 1.8-T, 8-pole wiggler on beam line 4-1 of the Stanford Synchrotron Radiation Laboratory in transmission mode for all the model minerals and for Ti in schorlomite. In the case of V in the schorlomite, measurements were made in the fluorescence mode using a Lytle detector (Lytle et al., 1984). Five fluorescence scans were acquired and averaged to improve the signal to noise ratio. A Si (220) double crystal monochromator was used, with no focusing optics, and a 1-mm upstream vertical aperture to produce a monochromatic synchrotron X-ray beam trimmed to dimensions of approximately 1 mm × 10 mm. The energy scales were calibrated relative to the first inflection point in either Ti or V foils as appropriate (4966.0 and 5465.0 eV, respectively).

Fe²⁺ determination

Fe²⁺ content was determined by titration against a standardized potassium permanganate solution after sample dissolution in a boiling mixture of sulfuric and hydrofluoric acids (modified after Groves, 1937). This

TABLE 1. Mineral standards used for synchrotron study

Mineral	Source	Formula
Vanadinite	Mibladen, Morocco	$Pb_5(VO_4)_3Cl$
Descloizite	Grootfontein Mine, Berg Aukas, Namibia	$PbZn(VO_4)OH$
Cavansite	Poona, Maharashtra, India	$Ca(VO)Si_4O_{10}\cdot4H_2O$
Titanite	Ice River Complex, Yoho National Park, British Columbia, Canada	$CaTiSiO_5$
Rutile	Ibitiara, Bahia, Brazil	TiO_2

volumetric procedure used a portion of the purified schorlomite separate that had been finely ground in an alumina ball mill with CO_2 pellets.

V present in the Ice River schorlomite was shown to be trivalent by XANES (see results section below). The presence of V³⁺ leads to an overestimation of Fe²⁺ (Groves, 1937). A correction was applied to the Fe²⁺ content using the V concentration determined by INAA. For the measured 0.20 wt% V_2O_3 content of the schorlomite, it was calculated that 0.38 wt% FeO must be subtracted from the FeO value initially determined by titration.

OH content

To determine the OH content of the specimen, a doubly polished wafer of schorlomite measuring 85 ± 3 μm in thickness (measured with a Logitech two-dial micrometer) was prepared and dried at 60 °C. Unpolarized FTIR spectra were recorded using a Nicolet 60SX spectrometer. The OH content was calculated using the absorption coefficient of Rossman and Aines (1991) for grossular with low OH content. Such a relationship has not yet been determined for schorlomite, but the absorption coefficient for grossular should give comparable results at these OH concentrations (Lager et al., 1989; Rossman, 1993 personal communication).

Mössbauer spectroscopy

Room-temperature Mössbauer (^{57}Fe) spectra were obtained for the unheated powdered sample, the unheated single crystal wafer, and the heated schorlomite powder using a nominal 50-mCi ^{57}Co source in Rh (1.85 GBq) at the University of Alberta. The amount of sample powder sandwiched between two layers of Mylar was adjusted to give an absorber thickness of ~5 mg Fe/cm² to avoid saturation effects (Bancroft, 1973). Mirror-image Mössbauer spectra were recorded using a microcomputer-based multi-channel analyzer. Between one and five million off-resonance counts per channel were collected. A velocity range of 4 mm/s was used; this velocity was calibrated with Fe foil, with values of $g_0 = 3.9156$ mm/s and $g_1 = 2.2363$ (Stevens and Stevens, 1972). The isomer shifts are reported relative to metallic Fe at room temperature.

Data from the two sides of the mirror-imaged spectrum were folded and then fitted with Lorentzian doublets by a least-squares procedure with the program PCMOS. Spectra of unheated schorlomite were fitted with equal area, equal half-width doublets for both Fe³⁺ and Fe²⁺.

TABLE 2. Physical parameters of Ice River schorlomite

Index of refraction, n	1.940
Density (g/cm³)	3.77*
	3.80**
Unit-cell dimension, a (Å)	12.153
Mohs hardness	6.5–7
X-ray lines (Å)	2.716(100)
	3.037(55)
	1.624(54)
	2.481(41)
	1.686(23)

Note: numbers in parentheses are relative intensities.
  * Mean of five measurements.
  ** Calculated with the cell dimension and chemical analysis.

TABLE 3. Chemical analysis and cation proportions of schorlomite

Oxide	Wt%	Cation	Atoms per 12 O	Trace elements	ppm
SiO_2	27.42(0.610)	Si	2.348(0.0402)	Sc	6.4(0.2)
TiO_2	16.43(0.852)	Ti	1.058(0.0463)	Cr	7.3(1.2)
ZrO_2	0.93(0.118)	Zr	0.039(0.0049)	Co	22.2(0.3)
Al_2O_3	1.36(0.139)	Al	0.137(0.0139)	Zn	218(10)
Fe_2O_3	15.05(0.546)	Fe^{3+}	0.970(0.0333)	Rb	25(5)
FeO	5.14(0.033)	Fe^{2+}	0.368(0.0055)	Sr	130(28)
V_2O_3	0.20(0.008)	V	0.014(0.0006)	Ba	247(12)
MnO	0.44(0.040)	Mn	0.032(0.0029)	La	68(2)
MgO	1.06(0.106)	Mg	0.135(0.0135)	Ce	321(8)
CaO	31.24(0.274)	Ca	2.866(0.0432)	Nd	377(10)
Na_2O	0.23(0.036)	Na	0.038(0.0060)	Sm	128(2)
H_2O^+	0.036(0.003)	H_4	0.005(0.0004)	Eu	58(1)
Rem*	0.25	Σ cations	8.010(0.0275)	Tb	27.4(0.3)
Total	99.79	Fe^{3+}/Fe_{tot}	0.725(0.031)	Dy	139(7)
				Yb	68(2)
				Lu	8.8(0.5)
				Hf	145(6)
				Ta	71(1)
				Th	31(1)
				U	35(1.5)

Note: numbers in parentheses represent a standard deviation of 1σ.
  * Rem = remainder, includes trace elements as oxides; lanthanides calculated as sesquioxides (R_2O_3).

The spectrum of heated schorlomite was fitted with equal area, equal half-width doublets for Fe^{3+} only, as Fe^{2+} was not detectable.

The 80-K spectrum was obtained through the courtesy of D. Canil at the Bayerisches Geoinstitut, Bayreuth, Germany. The apparatus is similar to that used for the room-temperature experiments at the University of Alberta; this spectrum was collected over a velocity range of 5 mm/s.

Infrared and optical spectroscopy

Room-temperature FTIR spectra in the region 1000–3000 nm were recorded on a Nicolet Nic-Plan Magna-IR 750 series microscope. Optical absorption spectra were recorded at room temperature using a Hewlett Packard 8450A spectrophotometer. Doubly polished sections of unheated and heated schorlomite mounted on glass slides with epoxy were examined.

RESULTS

The physical properties of the unheated Ice River schorlomite specimen are listed in Table 2. The refractive index and cell edge are in agreement with the values determined by Howie and Woolley (1968), and the measured and calculated densities agree with the more recent work of Wu and Mu (1986). The X-ray lines are very similar to those listed by JCPDS card 33-285 for schorlomite from Oka, Quebec, Canada.

In the heated powder sample, the schorlomite decomposed to a mixture of rutile, ferric oxide and a garnet with a slightly expanded unit cell (to 12.167 Å). The wafer of heated schorlomite was optically anisotropic and polycrystalline. However, the X-ray powder pattern could still be fitted to the space group $Ia3d$.

Chemical composition

The electron microprobe analyses of the schorlomite are given in Appendix Table 1. The degree of uniformity of the 33 analyses over an aggregate distance of 8250 μm is consistent with a homogeneous specimen. Therefore, unlike compositionally zoned garnets, bulk analytical techniques may be used upon different aliquots of this sample to determine additional aspects of its composition.

Table 3 lists the chemical analysis and calculated cat-

ion proportions of the schorlomite. The chemical data presented include the mean results of the microprobe analyses, the minor elements (including V) and trace elements measured by INAA, the Fe^{2+} content (the mean of five volumetric analyses) and the OH content (determined by FTIR, Fig. 1). The 1σ sd for the mean microprobe results and the mean volumetric Fe^{2+} content in Table 3 were calculated from the variations of the analyses. The standard deviations for the results of the other techniques were either derived from counting statistics and replicate analyses of standard materials (INAA) or estimated (FTIR).

The cation proportions of the major and minor elements, based on 12 O atoms, were calculated assuming divalent Mn; V was shown to be trivalent and Ti to be tetravalent by XANES (see below). The trace elements were excluded, as their contribution to the cation sum was calculated to be negligible. The Fe^{2+} content was taken from the corrected mean volumetric analysis, and the Fe^{3+} calculated by difference from the mean Fe_{tot} as determined from the microprobe analyses. The OH content was assumed to occur in the tetrahedral hydrogarnet substitution (Lager et al., 1989; Geiger et al., 1991), although it is possible that the OH may substitute in all three cation sites (Rossman and Aines, 1991). Uncertainties in the cation proportions and sum were calculated by partial error propagation methods (Giaramita and Day, 1990). The cation sum agrees within error to the stoichiometric value of 8 cations per 12 O atoms.

XANES

The element-specific technique of XANES provides information on valency, coordination and site symmetry
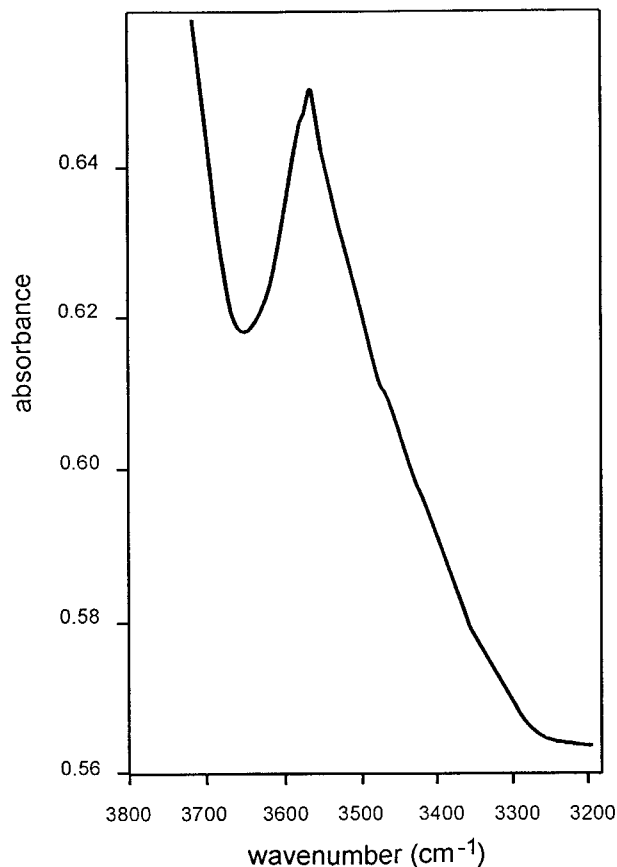
Fig. 1. Unpolarized infrared absorption spectrum of Ice River schorlomite (85 μm thick) showing the strongest peak at 3564 cm^{-1} attributed to OH.
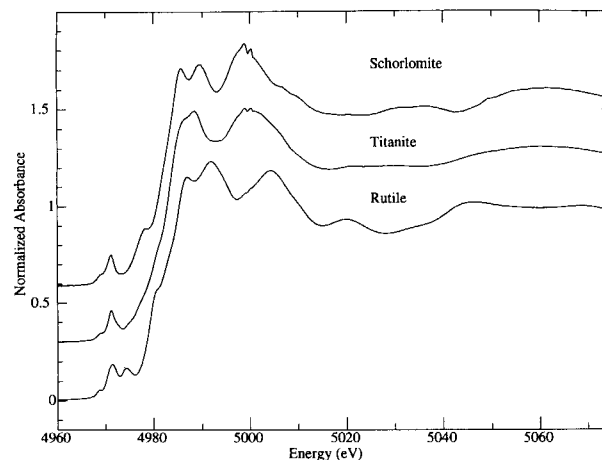

Fig. 2. Background-subtracted TiK edge X-ray absorption spectra for schorlomite and the model compounds titanite ([6]Ti^{4+}) and rutile ([6]Ti^{4+}). Fine structure at about 4999 eV is a mono-chromator crystal artifact.

(Henderson et al., 1993); however, current interpretation of XANES spectra is qualitative in nature (Brown and Parks, 1989). The similarity of XANES spectra for an unknown and a structurally well-characterized standard indicates that the absorber has the same coordination in both compounds (Brown and Parks, 1989).

The Ti XANES spectra shown in Figure 2 demonstrate the resemblance of the schorlomite spectrum to those of rutile and titanite. Analysis of the spectral features of these minerals (Table 4) shows them to be very similar to those reported previously for the same mineral species (Way-chunas, 1987; Henderson et al., 1993). These analogous spectra were interpreted as indicating the presence of [6]Ti^{4+} only [minor amounts, <10 at%, of other oxidation or coordination states would not be detectable by XANES (Waychunas, 1987) and would not affect the formula calculations within the propagated analytical error]. Consequently, the Ti in this specimen of schorlomite is considered to be present as [6]Ti^{4+}. The fine structure observed in the Ti spectra at about 4999 eV (Fig. 2) is a result of a monochromator crystal artifact.

The energies of the absorption features of [4]Ti^{4+} in Ba$_2$TiO$_4$ and a natural diopside sample are presented in Table 4, along with the spectral features of NaTi^{3+}Si$_2$O$_6$ and αTi$_2$O$_3$. Comparison of these spectral features with those of schorlomite indicates that neither [4]Ti^{4+} nor [6]Ti^{3+} is present in this schorlomite specimen.

The V XANES spectra are shown in Figure 3, and their peak parameters listed in Table 4. The spectrum of schorlomite was obtained by fluorescence methods because of its low V concentration, and, despite the relatively high noise level, the signal was of sufficient quality to determine the coordination and oxidation state of the V. The spectra of vanadinite and descloizite, which contain [4]V^{5+} (Hawthorne and Faggiani, 1979; Dai and Hughes, 1989), are quite similar to each other (Wong et al., 1984). The spectrum of cavansite, with V^{4+} in square-pyramidal co-ordination (Evans, 1973), corresponds well to spectra of other compounds containing V^{4+} in the same coordination (Wong et al., 1984).

The schorlomite V spectrum differs significantly from the V minerals, especially in the lack of a significant preedge peak. Instead, the schorlomite spectrum has peak energies (Table 4) similar to the spectra of roscoelite (V^{3+}-containing mica) and V$_2$O$_3$ (corundum structure), both of which contain [6]V^{3+} (Wong et al., 1984). The V in this specimen of schorlomite is therefore considered to be present as [6]V^{3+}.

Infrared spectroscopy

The infrared spectrum of the unheated doubly polished wafer of schorlomite shows an intense, broad asymmetric absorption (FWHM about 1850 cm^{-1}) estimated to be composed of two overlapping peaks centered at 1900 nm and 2300 nm, respectively (Fig. 4). The heated wafer does not show any peaks in that same region. This band has been reported previously in schorlomite and titanian an-dradite specimens (Manning and Harris, 1970; Moore and White, 1971; Dowty, 1971; Huggins et al., 1977b).

TABLE 4. Energies (eV) of Ti and V X-ray absorption features

Sample	Preedge features			Main-edge features		
	1	2	3	4	5	6
Ti spectra						
Titanite	4968.7	4971.2	*	4980.8	4984.5	4988.8
Rutile	4968.6	4971.4	4974.2	4980.3	4986.4	4991.9
Schorlomite	4968.6	4971.1	*	4978.0	4985.3	4989.5
Ba_2TiO_4,**	*	4967.8	*	4974.0	4979.5	4983.8
Diopside†	*	4967.8	*	4976.8	4981.1	4989.8
αTi_2O_3**	*	4967.7	*	4976.0	*	4985.5
$NaTi^{3+}Si_2O_6$**	4966.1	4967.3	4969.1	4976.5	4981.9	4987.3
V spectra						
Vanadinite	5469.7			*	5490.0	
Descloizite	5469.7			5483.2	5491.1	
Cavansite	5469.3			5476.8	5485.6	
Roscoelite‡	5467.6			5475.6	5486.5	
V_2O_3‡	5468.4			5475.7	5488.5	
Schorlomite	*			5476.0	5485.7	

* Feature too weak or ill-defined to be fitted.
** From Waychunas (1987), values reported relative to the first inflection point of Fe foil (7111.2 eV).
† Specimen D13 from Quartieri et al. (1993).
‡ From Wong et al. (1984).

Fig. 3. Background-subtracted VK edge X-ray absorption spectra for schorlomite and the model compounds vanadinite ($^{[4]}V^{5+}$), descloizite ($^{[4]}V^{5+}$), and cavansite ($^{[5]}V^{4+}$). The schorlomite spectrum was obtained by fluorescence techniques, and the model compound spectra were obtained by transmission methods. The step size in the fluorescence spectrum is smaller within the vicinity of absorption edge.

The position and width of this band are similar to those of bands observed in the γ-polarized absorption spectrum of staurolite (Burns, 1970) and in the Apollo 17 spinel 70002,7 (Mao and Bell, 1975). The interpretation of these bands is addressed below.

Mössbauer spectroscopy

Mössbauer spectroscopy was used to constrain the distribution of Fe and thereby indirectly to place limits on the positions of the other cations. Room-temperature spectra were acquired for an unheated powder sample ground in air, an unheated powder sample ground in the presence of solid CO_2, and an unheated doubly polished single-crystal wafer. The three spectra were identical (a representative spectrum, with valence and coordination assignments, is shown in Fig. 5). Fe^{2+} doublets were poorly resolved in the room-temperature spectra. Therefore a spectrum was acquired at 80 K of the unheated powder. Low-temperature spectra should be more accurate than 295-K spectra because the differences between the recoil-free fractions at the three nonequivalent sites in garnet decrease at lower temperatures, although the magnitude of the recoil-free fraction increases (Hawthorne, 1988; Kühberger et al., 1989). Figure 6 shows the 80-K spectrum with valence and coordination assignments for the various peaks. A room-temperature spectrum of the heated schorlomite powder was also acquired and is shown in Figure 7, with valence and coordination assignments (note than an undetermined proportion of the $^{[6]}Fe^{3+}$ should be assigned to ferric oxide that formed during the partial thermal decomposition of the schorlomite). The Mössbauer parameters for all these spectra and for the 80-K spectrum of a titanian andradite from Oberrotweil, Germany (From Kühberger et al., 1989) are listed in Table 5. The hyperfine parameters for the unheated Ice Riv-
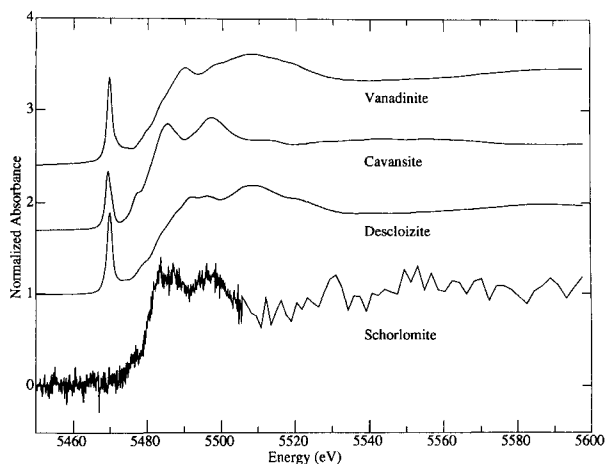
er schorlomite at low temperature are similar to those of the Oberrotweil titanian andradite. Note that the $^{[6]}Fe^{2+}$ doublet is a minor contributor to the absorption envelope, and therefore the position of the low-velocity peak is very poorly constrained. Of particular interest is the interpretation of $^{[4]}Fe^{2+}$ based upon the doublet with an isomer shift of 1.03 mm/s.

Optical spectroscopy

Figure 8 shows unpolarized optical absorption spectra for both the unheated and heated schorlomite specimens. Both spectra show a narrow, strong peak at about 440 nm, interpreted to be the most intense of the spin-forbidden transitions of $^{[6]}Fe^{3+}$, similar to that observed in the spectrum of andradite (Rossman, 1988). The intensity of the 440-nm band in the spectrum of the heated sample is a result of $^{[6]}Fe^{3+}$ in both the garnet structure and the accompanying ferric oxide. The unheated spectrum has a very broad intense band (FWHM approximately 8000 cm^{-1}) centered at about 500 nm. Similar features have been described previously in titanian andradite and schorlomite (Manning and Harris, 1970; Moore and White, 1971; Dowty, 1971; Huggins et al., 1977b). The width and position of this band resemble the Fe^{2+}-Ti^{4+} optically activated intervalence charge-transfer (IVCT) bands observed in neptunite, taramellite, and traskite (Mattson and Rossman, 1988).

DISCUSSION

$^{[4]}Fe^{2+}$

Tetrahedrally coordinated Fe^{2+}, although uncommon in minerals, is known to occur in members of the spinel group and in silicates such as staurolite and melilite
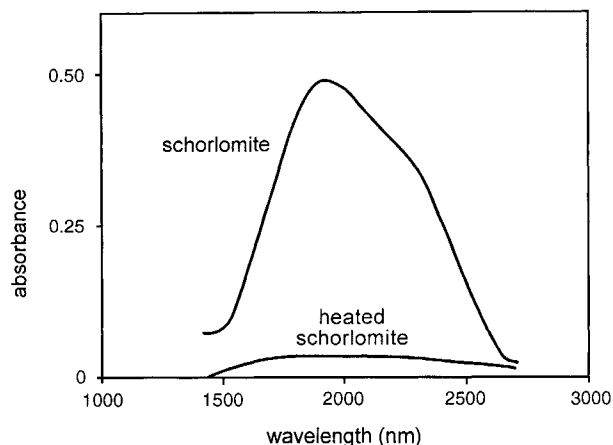
Fig. 4. Unpolarized near-infrared absorption spectra of schorlomite, 30 μm thick, and heated schorlomite, 50 μm thick.

Fig. 5. Mössbauer spectrum of ^{57}Fe in schorlomite, acquired at 295 K. The base line is 1.35×10^7 counts. The spectrum has been evaluated with four doublets. The size of the circles expresses the statistical uncertainty associated with each point. The velocity is referenced to the Fe in Rh source; add 0.11 mm/s to correct to velocity relative to Fe metal.

(Kühberger et al., 1989; Hawthorne et al., 1993). In this study, results from both infrared and Mössbauer spectroscopies are consistent with Fe^{2+} partially occupying the tetrahedral site in schorlomite.

The absence of the near-infrared band in the heated specimen of schorlomite (Fig. 4), implies that the band is related to the presence of a reduced species that was oxidized during the heat treatment. The width of the band (~ 1850 cm^{-1}) is within the typical range of crystal-field transitions (Smith, 1978; Langer, 1988). It closely resembles, in position and width, the near-infrared bands interpreted to represent $^{[4]}Fe^{2+}$ transitions, observed in staurolite and lunar spinel (Burns, 1970; Mao and Bell, 1975). Assignment of the band in schorlomite to dodecahedral Fe^{2+}-$^{[4]}Fe^{3+}$ electron delocalization or charge transfer (Schwartz et al., 1980; Platonov et al., 1991) is inconsistent with its narrow width. Charge-transfer transitions are characterized by their large half-widths, generally >4000 cm^{-1} (Mattson and Rossman, 1987a). The low-temperature behavior of the band precludes its interpretation as a regular crystal-field transition (Moore and White, 1971). The band increases in intensity and wavelength with decreasing temperature (Fig. 3 of Moore and White, 1971) and has therefore been interpreted as a spin-allowed crystal-field transition of $^{[4]}Fe^{2+}$, intensified by coupling with adjacent Fe^{3+} (Smith, 1978). Similar intensified spin-allowed transitions of $^{[6]}Fe^{2+}$ have been recognized in iron magnesium tourmalines, biotite, and partially oxidized vivianite (Smith, 1978; Mattson and Rossman, 1987b; Rossman, 1988). The theory behind the intensification of the Fe^{2+} transitions by coupling with Fe^{3+} is still being developed (Sherman, 1987a; Rossman, 1988). The asymmetry (splitting) of the infrared Fe^{2+} band in schorlomite is a result of the distorted nature of the fourfold-coordinated site in the garnet structure, a tetragonal disphenoid, point group $\bar{4}$ (S_4 in Schoenflies notation), in comparison with the regular tetrahedron of spinel, point group $\bar{4}3m$ (T_d in Schoenflies notation) (Meagher, 1982; Jaffe, 1988; Rossman, 1988).
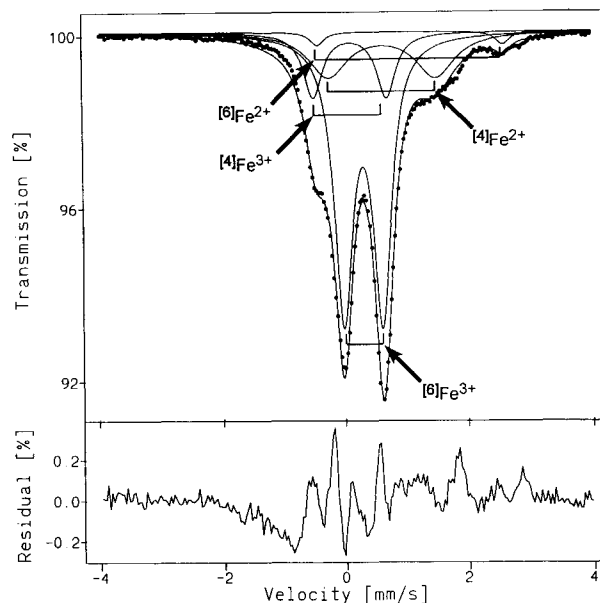
The Mössbauer spectra of Ti-rich andradite and schorlomite are more complex than those of most of the chemically simpler garnets (Hawthorne, 1988). In the Ti-rich garnets, the presence of Fe^{3+} in both tetrahedral and octahedral coordination as well as $^{[6]}Fe^{2+}$, are well established. Dodecahedral Fe^{2+} may be absent depending on the chemistry of the particular specimen examined. However, the assignment of $^{[4]}Fe^{2+}$ based on Mössbauer spectroscopy has caused considerable controversy. In accordance with the Mössbauer parameters determined (using constrained doublets) for titanian andradite by Kühberger et al. (1989), the peak with the quadrupole splitting of 2.27 mm/s and isomer shift of 1.03 mm/s is assigned to $^{[4]}Fe^{2+}$ (Table 5). This isomer shift is similar to the average value of 0.98 mm/s for Fe^{2+} observed in the three tetrahedral subsites of staurolite (Dyar et al., 1991). The large temperature dependence of the quadrupole splitting of this peak in schorlomite (-0.0024 mm/sK in this study; -0.0017 mm/sK: Amthauer et al., 1977; Kühberger et al., 1989) has been interpreted as evidence for electron delocalization (thermally activated charge transfer), instead of $^{[4]}Fe^{2+}$ (Schwartz et al., 1980; Yupu and Ruiying, 1985; Wu and Mu, 1986). The lack of anomalous Mössbauer parameters indicates that no electron delocalization is taking place (Amthauer et al., 1977; Hawthorne, 1988; Kühberger et al., 1989). For Fe^{2+}-Fe^{3+} electron delocalization to occur, the Fe sites would have to form punctuated chains, sheets, or networks (Sherman, 1987a). This requirement is not met by the garnet structure. In addition, high-spin Fe^{2+} is expected to show tempera-

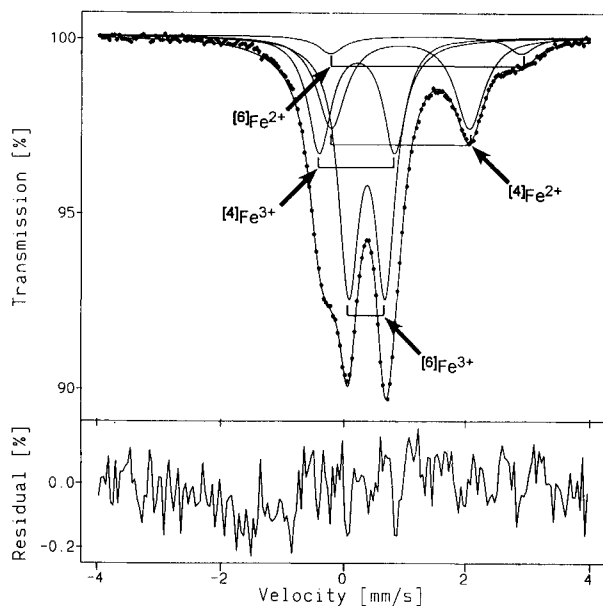Fig. 6. Mössbauer spectrum of ^{57}Fe in schorlomite, taken at 80 K. The base line is 2.68 × 10^6 counts. The spectrum has been evaluated with four doublets. The velocity is referenced to the Fe in Rh source; add 0.11 mm/s to correct to velocity relative to Fe metal.
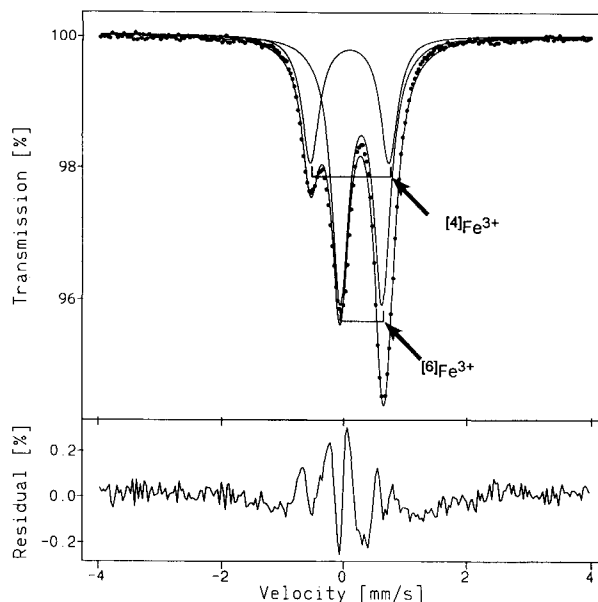
Fig. 7. Mössbauer spectrum of ^{57}Fe in heated schorlomite, acquired at 295 K. The baseline is 1.52 × 10^7 counts. The spectrum has been evaluated with two doublets. The velocity is referenced to the Fe in Rh source; add 0.11 mm/s to correct to velocity relative to Fe metal.

ture-dependent quadropole splitting, as a result of its electronic state in the distorted tetrahedral site of the garnet structure (Amthauer et al., 1977; Hawthorne, 1988).

Site occupancies

With the constraints provided by XANES, Mössbauer, and near-infrared spectroscopies, the distribution of cation species (assuming no vacancies) between the three sites in schorlomite may be calculated (Table 6). In accordance with the usual crystal chemistry of the garnet structure, all the Ca and Na are allocated to the dodecahedral site. No dodecahedral Fe^{2+} was observed with low-

temperature Mössbauer spectroscopy; therefore the remainder of the dodecahedral site is filled with Mg and Mn. However, more Mn and Mg are present than are required to fill the dodecahedral site. The excess should occur in octahedral coordination by analogy with the isostructural berzeliite-manganberzeliite series: $\{Ca,Na\}_3$ $[Mg,Mn]_2(As)_3O_{12}$-$\{Ca,Na\}_3[Mn,Mg]_2(As)_3O_{12}$. The ratio of Mn to Mg is assumed to be the same in the dodecahedral and octahedral sites in Ice River schorlomite because the partitioning behavior of either element between the two sites is uncertain. The evidence from XANES indicates that all the Ti is tetravalent, all the V is triva-

TABLE 5. Mössbauer parameters of ^{57}Fe in schorlomite

Sample	T (K)	x^2	Valence and site	QS (mm/s)	IS (mm/s)	Width (mm/s)	Area (%)
I90.4sch (UA0060)	295	9.95	$^{[4]}Fe^{3+}$	1.21	0.21	0.38	15.0
			$^{[6]}Fe^{3+}$	0.64	0.41	0.37	61.5
			$^{[4]}Fe^{2+}$	1.76	0.74	0.78	21.1
			$^{[6]}Fe^{2+}$	3.03	1.19	0.29	2.4
I90.4sch (BY1374M)	80	1.78	$^{[4]}Fe^{3+}$	1.24	0.32	0.43	24.8
			$^{[6]}Fe^{3+}$	0.60	0.49	0.41	46.1
			$^{[4]}Fe^{2+}$	2.27	1.03	0.57	24.5
			$^{[6]}Fe^{2+}$	3.12	1.44	0.53	4.5
Oberrotweil	80	0.57	$^{[4]}Fe^{3+}$	1.28	0.37	0.43	21.9
			$^{[6]}Fe^{3+}$	0.64	0.51	0.38	61.3
			$^{[4]}Fe^{2+}$	2.11	1.03	0.48	8.6
			$^{[6]}Fe^{2+}$	3.26	1.22	0.33	4.7
			$^{[8]}Fe^{2+}$	3.64	1.39	0.24	3.4
I90.4sch (UA0067 ox)	295	8.17	$^{[4]}Fe^{3+}$	1.28	0.21	0.34	33.2
			$^{[6]}Fe^{3+}$	0.69	0.40	0.34	66.8

Note: x^2 per channel; QS = quadropole splitting; IS = isomer shift relative to Fe metal at 298 K; width = full width at half maximum peak height; area = fractional area beneath resonant envelope; I90.4sch = schorlomite from this study; UA0060 = 295-K spectrum recorded at the University of Alberta; BY1374M = 80-K spectrum recorded Bayerisches Geoinstitut; Oberrotweil = data from Kühberger et al. (1989); UA0067 ox = 295-K spectrum recorded at the University of Alberta upon the heated (oxidized) sample. The oxidized sample was heated at 1050 °C in air for 594 h.
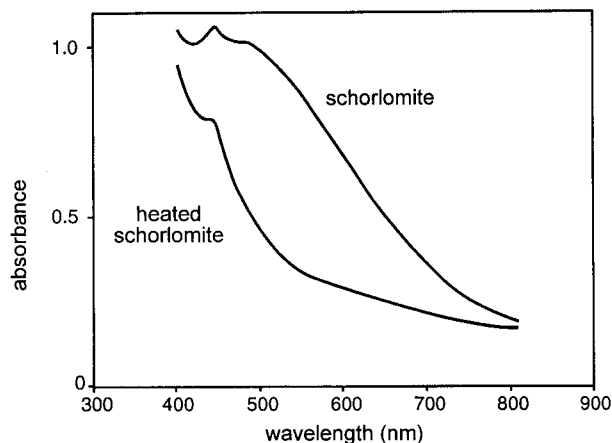
Fig. 8. Unpolarized optical absorption spectra of schorlomite, 10 μm thick, and heated schorlomite, 50 μm thick.

TABLE 6. Cation distribution of Ice River schorlomite

Cation	Atoms per 12 O	Crystallographic site		
		Dodec.	Oct.	Tet.
Si	2.348			2.348
Ti	1.058		1.058	
Zr	0.039		0.039	
Al	0.137		0.137	
Fe^{3+}	0.970		0.631	0.339
Fe^{2+}	0.368		0.057	0.311
V^{3+}	0.014		0.014	
Mn	0.032	0.019	0.013	
Mg	0.135	0.080	0.055	
Ca	2.866	2.866		
Na	0.038	0.038		
H$_4$	0.005			0.005
Total	8.010	3.003	2.004	3.003

lent, and both are in octahedral coordination. Zr is assigned to the octahedral site, as in the kimzeyite species of garnet $\{Ca\}_3[Zr,Ti]_2(Si,Al,Fe^{3+})_3O_{12}$. The Fe^{2+} (from the corrected mean volumetric analysis) and the Fe^{3+} are distributed between the octahedral and tetrahedral sites on the basis of the 80-K Mössbauer results. All the Al must be assigned to the octahedral site in order to fill it. The tetrahedral site is occupied by Si, the Fe^{3+} and Fe^{2+} allocated on the basis of Mössbauer spectroscopy, and H (assumed to occur as OH in the hydrogarnet substitution). Neither Al nor Ti is required to fill the tetrahedral site. The presence of substantial $^{[4]}$Fe (both Fe^{3+} and Fe^{2+}) may give rise to an additional distinct tetrahedral site in the garnet structure, an Fe tetrahedron as well as the Si tetrahedron (single-crystal structure refinement: Peterson, unpublished material). The order of occupancy for the tetrahedral site (after Si and without OH) based on the above data is Fe^{3+} > Fe^{2+} ≫ Al,Ti in contrast to the assignments made by Huggins et al. (1977a): Al ≥ Fe > Ti, and Schwartz et al. (1980): Fe^{3+} > Al,Ti^{4+}. This sequence may be influenced by the bulk chemical composition of the individual specimens examined.

Unlike other chemical variations within natural garnets, no single substitution can account for the presence of tetravalent cations (Ti and Zr) in the octahedral site of schorlomite because of their high concentrations. Given the cation distribution from Table 6 and assuming that the andradite-schorlomite series contains the cation components Na$^+$, Ca^{2+}, Fe^{2+}, Fe^{3+}, Ti^{4+}, and Si^{4+} (homovalent cations can be treated as one of the above, i.e., Al^{3+} instead of Fe^{3+}), the following coupled substitutions may be written: $^{[8]}$Na + $^{[6]}$Ti ⇌ $^{[8]}$Ca + $^{[6]}$Fe^{3+}; $^{[6]}$Ti + $^{[6]}$Fe^2 ⇌ $^{[6]}$Fe$_2^{3+}$; $^{[6]}$Ti + $^{[4]}$Fe^{3+} ⇌ $^{[6]}$Fe^{3+} + $^{[4]}$Si; $^{[6]}$Ti$_2$ + $^{[4]}$Fe^{2+} ⇌ $^{[6]}$Fe$_2^{3+}$ + $^{[4]}$Si.

Schorlomite has often been thought to contain Ti^{3+}. Previous workers have used two methods to calculate the amount of Ti^{3+} present. One method was to normalize the cation sum to exactly 8 cations per 12 O atoms by adjusting the Ti^{3+}-Ti$_{tot}$ ratio (after the Fe^{3+}-Fe$_{tot}$ ratio had

been determined). The other technique was to compare the Fe^{3+}-Fe$_{tot}$ ratio determined by titration with that measured by Mössbauer spectroscopy; the difference between these was taken to indicate the reducing presence of Ti^{3+} in the wet-chemical determination. Ti^{3+} is not required in the calculated cation distribution listed in Table 6. The cation sum agrees within 1σ analytical uncertainty, with the stoichiometric value of 8 cations per 12 O atoms (Table 3). Consequently no Ti^{3+} can be calculated on the basis of charge-balance considerations. The Fe^{3+}-Fe$_{tot}$ ratio from the mean corrected volumetric determination (0.725 ± 0.031) agrees within 1σ error with that measured by 80-K Mössbauer spectroscopy (0.710 ± 0.008). This implies that the only reduced cations present are Fe^{2+} (and V^{3+}, as shown by XANES).

Intervalence charge transfer

Intervalence charge-transfer (IVCT) transitions result from the movement of electron density from one metal cation to another that is in a different oxidation state (Rossman, 1988). The cations interact with each other either by direct orbital overlap across shared edges or faces of coordination polyhedra or by metal-ligand-metal super-exchange across a shared corner (Sherman, 1987a; Rossman, 1988; Hawthorne et al., 1993). IVCT transitions are usually optically induced and give absorption bands in the visible and near-infrared regions (Sherman, 1987a). In some minerals with infinite octahedral chains containing Fe^{2+} and Fe^{3+}, Fe^{2+}-Fe^{3+} IVCT is thermally induced and can be observed using Mössbauer spectroscopy (Sherman, 1987a; Hawthorne, 1988).

The wide band (~8000 cm^{-1}) centered at 500 nm in the optical absorption spectrum of schorlomite (Fig. 8) can be assigned to Fe^{2+}-Ti^{4+} IVCT. This band has a sufficiently large width (Mattson and Rossman, 1987a) and is within the normal energy range of Fe^{2+}-Ti^{4+} charge-transfer transitions (Sherman, 1987b; Mattson and Rossman, 1988; Platonov et al., 1991).

In Ice River schorlomite, Ti is in octahedral coordination, the majority of the Fe^{2+} is assigned to the tetrahedral site, and the remainder is assigned to the octahedral site; no Fe^{2+} is present in the dodecahedral site (Table

6). Therefore, Fe^{2+}-Ti^{4+} charge transfer must take place by metal-ligand-metal super-exchange across the shared corner between [4]Fe^{2+} and [6]Ti^{4+}. The octahedra in the garnet structure do not share any common ligands, obviating any possibility of charge transfer between them.

Most Fe^{2+}-Ti^{4+} charge transfer transitions in silicate minerals take place across shared polyhedral edges or faces. The mineral traskite, however, has been described as exhibiting Fe^{2+}-Ti^{4+} IVCT, and the Fe and Ti in its structure share only corners in three-fourths of its octahedra (Mattson and Rossman, 1988).

Fe^{2+}-Ti^{4+} charge transfer has been described in pyrope-grossular-almandine garnets from mantle eclogites (Platonov et al., 1991; Langer et al., 1993). Unlike the schorlomite discussed in this paper, the mantle garnets show a broad band ($\sim$7000 cm^{-1}) centered between 425 and 465 nm. The Fe^{2+} in these garnets is entirely in dodecahedral coordination (on the basis of Mössbauer spectroscopy), and the Ti is assumed to be in octahedral coordination, as there is sufficient Si to fill the tetrahedral site. Therefore, the Fe^{2+}-Ti^{4+} charge transfer takes place across the shared edge between Fe^{2+} in dodecahedral coordination and [6]Ti. The difference in energy (wavelength) between the transition in schorlomite and the transitions in the mantle garnets can be attributed to the different crystallographic sites occupied by the Fe^{2+}. According to Sherman (1987a), when cations occupy crystallographically dissimilar sites they experience different electrostatic potentials, and these potential energies affect the energy of the IVCT.

Despite the presence of substantial Fe^{3+} and Fe^{2+} in both the octahedral and tetrahedral sites of schorlomite, no indication of Fe^{2+}-Fe^{3+} IVCT was observed by optical absorption spectroscopy (Fig. 8). It is probable that the Fe^{2+}-Fe^{3+} IVCT is buried in the optical spectrum beneath the more intense Fe^{2+}-Ti^{4+} IVCT.

ACKNOWLEDGMENTS

APPENDIX TABLE 1.   Electron microprobe analyses of Ice River schorlomite

	SiO_2	TiO_2	ZrO_2	Al_2O_3	Fe_2O_3*	MnO	MgO	CaO	Na_2O	Total
1	28.22	15.00	0.91	1.04	21.54	0.46	0.81	31.75	0.30	100.03
2	28.70	14.19	0.77	1.37	21.55	0.36	0.82	31.72	0.17	99.65
3	28.12	15.23	0.83	1.07	21.65	0.43	0.82	31.52	0.25	99.92
4	28.06	15.45	0.82	1.20	21.43	0.44	0.99	30.80	0.29	99.48
5	28.20	14.87	0.93	1.11	21.94	0.49	0.94	30.95	0.24	99.67
6	28.41	15.16	0.84	1.21	21.83	0.48	1.01	30.94	0.22	100.10
7	28.79	15.06	0.68	1.21	21.57	0.48	0.98	31.48	0.27	100.52
8	28.76	14.89	1.06	1.00	21.69	0.35	0.86	31.45	0.22	100.28
9	27.62	16.98	0.94	1.37	20.71	0.43	1.09	31.51	0.24	100.89
10	27.20	16.99	1.05	1.35	20.25	0.42	1.10	31.29	0.25	99.90
11	27.41	16.71	0.79	1.48	20.35	0.47	0.99	30.98	0.27	99.45
12	27.10	16.88	0.94	1.41	20.77	0.45	1.17	31.38	0.20	100.30
13	27.05	17.18	0.93	1.42	20.03	0.46	1.14	31.39	0.27	99.87
14	27.05	16.83	0.82	1.43	20.51	0.43	1.16	31.19	0.18	99.60
15	27.34	17.02	1.03	1.50	20.69	0.44	1.04	31.29	0.24	100.59
16	27.00	16.69	0.97	1.42	20.67	0.42	1.12	31.56	0.26	100.11
17	27.29	16.84	0.85	1.43	20.73	0.37	1.14	31.07	0.23	99.95
18	27.05	16.94	0.96	1.42	20.24	0.35	1.10	30.94	0.13	99.13
19	26.98	16.86	0.95	1.47	20.56	0.38	1.06	30.96	0.25	99.47
20	26.96	16.86	0.91	1.41	20.61	0.47	1.11	31.26	0.25	99.84
21	27.35	16.84	1.18	1.46	20.62	0.49	1.08	31.14	0.21	100.37
22	27.24	16.89	0.72	1.48	20.26	0.46	1.15	31.21	0.23	99.64
23	27.01	16.90	1.02	1.51	20.60	0.46	1.14	31.24	0.22	100.10
24	27.06	16.82	1.14	1.45	20.21	0.47	1.08	31.44	0.25	99.92
25	27.09	17.02	1.09	1.39	20.31	0.44	1.17	30.80	0.25	99.56
26	26.81	16.83	1.00	1.38	20.52	0.45	1.13	30.59	0.24	98.95
27	27.00	16.86	0.92	1.37	20.52	0.44	1.08	31.11	0.21	99.51
28	26.87	16.94	1.00	1.45	20.73	0.45	1.11	31.48	0.23	100.26
29	26.93	16.78	1.01	1.47	20.59	0.44	1.06	31.41	0.18	99.87
30	26.90	16.88	0.74	1.39	20.61	0.46	1.14	31.31	0.25	99.68
31	27.18	16.81	0.92	1.41	20.48	0.40	1.18	31.09	0.22	99.69
32	27.01	16.92	0.99	1.38	20.18	0.39	1.08	31.20	0.18	99.33
33	26.95	16.93	0.85	1.49	20.29	0.49	1.14	31.51	0.23	99.88

* Total Fe presented as Fe^{3+}.

REFERENCES CITED

Amthauer, G., Annersten, H., and Hafner, S.S. (1977) The Mössbauer spectrum of ^{57}Fe in titanium-bearing andradites. Physics and Chemistry of Minerals, 1, 399–413.

Appleman, D.E., and Evans, H.T., Jr. (1973) Job 9214: Indexing and least-squares refinement of powder diffraction data. U.S. National Technical Information Service, Document PB 216 188.

Bancroft, G.M. (1973) Mössbauer spectroscopy: An introduction for inorganic chemistry and geochemists, 252 p. Wiley, New York.

Basso, R., Giusta, A.D., and Zefiro, L. (1981) A crystal chemical study of a Ti-containing hydrogarnet. Neues Jahrbuch für Mineralogie Monatshefte, 5, 230–236.

Benoit, P.H. (1987) Adaptation to microcomputer of the Appleman-Evans program for indexing and least-squares refinement of powder-diffraction data for unit-cell dimensions. American Mineralogist, 72, 1018–1019.

Bergerioux, C., Kennedy, G., and Zikovsky, L. (1979) Use of the semi-absolute method in neutron activation analysis. Journal of Radioanalytical Chemistry, 50, 229.

Brown, G.E., Jr., and Parks, G.A. (1989) Synchrotron-based X-ray absorption studies of cation environments in earth materials. Reviews of Geophysics, 27, 519–533.

Burns, R.G. (1970) Mineralogical applications of crystal field theory, 224 p. Cambridge University Press, Cambridge, U.K.

Dai, Y., and Hughes, J.M. (1989) Crystal-structure refinements of vanadinite and pyromorphite. Canadian Mineralogist, 27, 189–192.

Deer, W.A., Howie, R.A., and Zussman, J. (1982) Andradite. In Rock-forming minerals, vol. 1A: Orthosilicates (2nd edition), p. 617–641. Longman, London.

de Groot, F.M.F., Figueiredo, M.O., Basto, M.J., Abbate, M., Petersen, H., and Fuggle, J.C. (1992) 2p X-ray absorption of titanium in minerals. Physics and Chemistry of Minerals, 19, 140–147.

Dingwell, D.B., and Brearley, M. (1985) Mineral chemistry of igneous melanite garnets from analcite-bearing volcanic rocks, Alberta, Canada. Contributions to Mineralogy and Petrology, 90, 29–35.

Dowty, E. (1971) Crystal chemistry of titanian and zirconian garnet: I. Review and spectral studies. American Mineralogist, 56, 1983–2009.

Dyar, M.D., Perry, C.L., Rebbert, C.R., Dutrow, B.L., Holdaway, M.J., and Lang, H.M. (1991) Mössbauer spectroscopy of synthetic and naturally occurring staurolite. American Mineralogist, 76, 27–41.

Evans, H.T., Jr. (1973) The crystal structures of cavansite and pentagonite. American Mineralogist, 58, 412–424.

Geiger, C.A., Langer, K., Bell, D.R., Rossman, G.R., and Winkler, B. (1991) The hydroxide component in synthetic pyrope. American Mineralogist, 76, 49–59.

Giaramita, M.J., and Day, H.W. (1990) Error propagation in calculations of structural formulas. American Mineralogist, 75, 170–182.

Groves, A.W. (1937) Silicate analysis, 230 p. Nordemann, New York.

Hawthorne, F.C. (1981) Some systematics of the garnet structure. Journal of Solid State Chemistry, 37, 157–164.

——— (1988) Mössbauer spectroscopy. In Mineralogical Society of America Reviews in Mineralogy, 18, 255–340.

Hawthorne, F.C., and Faggiani, R. (1979) Refinement of the structure of descloizite. Acta Crystallographica, B35, 717–720.

Hawthorne, F.C., Ungaretti, L., Oberti, R., Caucia, F., and Callegari, A. (1993) The crystal chemistry of staurolite: I. Crystal structure and site populations. Canadian Mineralogist, 31, 551–582.

Henderson, C.M.B., Charnock, J.M., Smith, J.V., and Greaves, G.N. (1993) X-ray absorption spectroscopy of Fe, Mn, Zn, and Ti structural environments in staurolite. American Mineralogist, 78, 477–485.

Hoffmann, G.C. (1902) Report of the section of chemistry and mineralogy. Geological Survey of Canada Annual Report, vol. 12, 12R–13R.

Howie, R.A, and Woolley, A.R. (1968) The role of titanium and the effect of TiO$_2$ on the cell-size, refractive index, and specific gravity in the andradite-melanite-schorlomite series. Mineralogical Magazine, 36, 775–790.

Huggins, F.E., Virgo, D., and Huckenholz, H.G. (1977a) Titanium-containing silicate garnets: I. The distribution of Al, Fe^{3+}, and Ti^{4+} between octahedral and tetrahedral sites. American Mineralogist, 62, 475–490.

——— (1977b) Titanium-containing silicate garnets: II. The crystal chemistry of melanites and schorlomites. American Mineralogist, 62, 646–665.

Jaffe, H.W. (1988) Crystal chemistry and refractivity, 335 p. Cambridge University Press, Cambridge, U.K.

Koenig, G.A. (1886) On schorlomite as a variety of melanite. Proceedings of the Academy of Natural Sciences of Philadelphia, 355–357.

Koritnig, S., Rösch, H., Schneider, A., and Seifert, F. (1978) Der Titan-Zirkon-Granat aus den Kalksilikatfels-Einschlüssen des Gabbro im Radautal, Harz, Bundesrepublik Deutschland. Tschermaks mineralogische-petrographische Mitteilungen, 25, 305–313.

Kühberger, A., Fehr, T., Huckenholz, H.G., and Amthauer, G. (1989) Crystal chemistry of a natural schorlomite and Ti-andradites synthesized at different oxygen fugacities. Physics and Chemistry of Minerals, 16, 734–740.

Lager, G.A., Armbruster, T., Rotella, F.J., and Rossman, G.R. (1989) OH substitution in garnets: X-ray and neutron diffraction, infrared, and geometric-modeling studies. American Mineralogist, 74, 840–851.

Langer, K. (1988) UV to NIR spectra of silicate minerals obtained by microscope spectrometry and their use in mineral thermodynamics and kinetics. In E.K.H. Salje, Ed., Physical properties and thermodynamic behavior of minerals, p. 639–650. Reidel, Boston.

Langer, K., Robarick, E., Sobolev, N.V., Shatsky, V.S., and Wang, W. (1993) Single-crystal spectra of garnets from diamondiferous high-pressure metamorphic rocks from Kazakhstan: Indications for OH$-$, H$_2$O, and FeTi charge transfer. European Journal of Mineralogy, 5, 1091–1100.

Leigh, G.J., Ed. (1990) Nomenclature of inorganic chemistry, 289 p. International Union of Pure and Applied Chemistry, Blackwell Scientific Publications, London.

Lueck, B.A., and Russell, J.K. (1994) Phenocrystic and cumulate melanite garnet: Substitution mechanisms and petrogenesis. Geological Association of Canada and Mineralogical Association of Canada Program with Abstracts, A67.

Lytle, F., Sandstrom, D.R., Marques, E.C., Wong, J., Spiro, C.L., Huffman, G.P., and Huggins, F.E. (1984) Measurement of soft X-ray absorption spectra with a fluorescent ion chamber detector. Nuclear Instrumental Methods, 226, 542–548.

Manning, P.G., and Harris, D.C. (1970) Optical-absorption and electron-microprobe studies of some high-Ti andradites. Canadian Mineralogist, 10, 260–271.

Mao, H.K., and Bell, P.M. (1975) Crystal-field effects in spinel: Oxidation states of iron and chromium. Geochimica et Cosmochimica Acta, 39, 865–874.

Mattson, S.M., and Rossman, G.R. (1987a) Identifying characteristics of charge transfer transitions in minerals. Physics and Chemistry of Minerals, 14, 94–99.

——— (1987b) Fe^{2+}-Fe^{3+} interactions in tourmaline. Physics and Chemistry of Minerals, 14, 163–171.

——— (1988) Fe^{2+}-Ti^{4+} charge transfer in stoichiometric Fe^{2+}, Ti^{4+}-minerals. Physics and Chemistry of Minerals, 16, 78–82.

Meagher, E.P. (1982) Silicate garnets. In Mineralogical Society of America Reviews in Mineralogy (2nd edition), 5, 25–66.

Moore, R.K., and White, W.B. (1971) Intervalence electron transfer effects in the spectra of the melanite garnets. American Mineralogist, 56, 826–840.

Onuki, H., Yoshida, T., and Nedachi, M. (1981) Electron probe study of Ti-rich hydroandradites in the Sanbagawa metamorphic rocks. Journal of the Japanese Association of Mineralogists, Petrologists and Economic Geologists, 76, 239–247.

Onuki, H., Akasaka, M., Yoshida, T., and Nedachi, M. (1982) Ti-rich hydroandradites from the Sanbagawa metamorphic rocks of the Shibukawa Area, Central Japan. Contributions to Mineralogy and Petrology, 80, 183–188.

Platonov, A.N., Langer, K., Matsuk, S.S., Taran, M.N., and Hu, X. (1991) Fe^{2+}-Ti^{4+} charge-transfer in garnets from mantle eclogites. European Journal of Mineralogy, 3, 19–26.

Quartieri, S., Antonioli, G., Artioli, G., and Lottici, P.P. (1993) XANES study of titanium coordination in natural diopsidic pyroxenes. European Journal of Mineralogy, 5, 1101–1109.

Rossman, G.R. (1988) Optical spectroscopy. In Mineralogical Society of America Reviews in Mineralogy, 18, 207–254.

Rossman, G.R, and Aines, R.D. (1991) The hydrous components in garnets: Grossular-hydrogrossular. American Mineralogist, 76, 1153–1164.

Sawaki, T. (1988) Melanite and fassaite from the contact aureole around the Nogo-Hakusan granodiorite body, central Japan. Journal of Mineralogy, Petrology and Economic Geology, 83, 357–373.

Schwartz, K.B., Nolet, D.A., and Burns, R.G. (1980) Mössbauer spectroscopy and crystal chemistry of natural Fe-Ti garnets. American Mineralogist, 65, 142–153.

Sherman, D.M. (1987a) Molecular orbital (SCF-Xα-SW) theory of metal-metal charge transfer processes in minerals: I. Application to $Fe^{2+}{\rightarrow}Fe^{3+}$ charge transfer and "electron delocalization" in mixed-valence iron oxides and silicates. Physics and Chemistry of Minerals, 14, 355–363.

——(1987b) Molecular orbital (SCF-Xα-SW) theory of metal-metal charge transfer processes in minerals: II. Application to $Fe^{2+}{\rightarrow}Ti^{4+}$ charge transfer transitions in oxides and silicates. Physics and Chemistry of Minerals, 14, 364–367.

Smith, G. (1978) Evidence for absorption by exchange-coupled Fe^{2+}-Fe^{3+} pairs in the near infra-red spectra of minerals. Physics and Chemistry of Minerals, 3, 375–383.

Stevens, I.G., and Stevens, V.E. (1972) Mössbauer effect data index, covering the 1970 literature, 369 p. IFI/Plenum Data, New York.

Waychunas, G.A. (1987) Synchrotron radiation XANES spectroscopy of Ti in minerals: Effects of Ti bonding distances, Ti valence, and site geometry on absorption edge structure. American Mineralogist, 72, 89–101.

Wong, J., Lytle, R.W., Messmer, R.P., and Maylotte, D.H. (1984) K-edge absorption spectra of selected vanadium compounds. Physical Review B, 30, 5596–5610.

Wu, G., and Mu, B. (1986) The crystal chemistry and Mössbauer study of schorlomite. Physics and Chemistry of Minerals, 13, 198–205.

Yupu, T., and Ruiying, C. (1985) An anomalous Mössbauer spectrum of schorlomite. Scientia Sinica, 28, 202–209.